Numerical modelling and analysis of the double pendulum motion

Marcin Jastrzebski, MPhys Physics with Particle Physics and Cosmology

PHYS389: Computer Modelling, Lancaster University Physics Department

Academic Year 2019/2020

Abstract

The 4th order Runge-Kutta method is used to perform simulations of double pendulums. A set of tools is created allowing for analysis of the properties of such systems. The phenomenon of beats in the small angle regime is investigated and shown to become more prominent with increasing pendulum mass ratio. Two cases with a difference of 0.05 radians in the initial displacement of one of the pendulum bobs are shown to start diverging significantly after 6 seconds as an example of deterministic chaos. A qualitative analysis of the paths created in phase space leads to the description of 5 motion types. Intricate dynamics of the system can be seen. An energy range for each of the categories is found. A colour map for the time it takes for one of the pendulums to flip is plotted along with an estimate of the numerical precision of the program using a theoretical symmetry postulate.

Contents

1 Introduction

A chaotic system's most prominent feature is its sensitivity to initial conditions [1] resulting in the lack of predictability. The study of chaos theory tackles problems like the limits of determinism in science and proves important in climate modelling [2], stock market analysis [3], or investigations of the Earth's interior [3]. In this report, the double pendulum is described as an example of a system displaying chaotic behaviour. The code developed by the author could be used as an analysis tool, introducing the user to chaos theory and the intricate dynamics of this seemingly simple system.

Section 2 describes the theory behind the motion of the double pendulum. Software details and the description of the numerical method used make up Sec. 3. A summary of simple tests of the code and some of its shortcomings can be found in Sec. 4. Finally, we investigate the rich dynamical behaviour of the system in Sec. 5, including an analysis of the small angle regime, different manifestations of chaos and a qualitative categorisation of the possible outcomes with relation to the total energy. The key findings of this experiment are summarised in Section 6.

2 Background

The double pendulum considered in this report consists of two simple pendulums made up of a *massless* rigid rod of length l and a bob of mass m attached to it. First pendulum is attached to the origin $(0, 0)$. The second - to the bob of the first. The dynamics happen in one plane (This is a 2-dimensional problem), in a constant gravitational field with acceleration g which we set to 10 for simplicity. Figure 1 illustrates this set up.

Angles θ_1 and θ_2 measure the deviation from the vertical for the first and second pendulum respectively. No friction on the pivot points or air resistance is assumed. The coordinates of the pendulums can be found with:

$$x_1 = l_1 sin\theta_1, \tag{2.1}$$

$$x_2 = l_1 sin\theta_1 + l_2 sin\theta_2, \tag{2.2}$$

$$y_1 = -l_1 cos\theta_1, \tag{2.3}$$

$$y_2 = -l_1 cos\theta_1 - l_2 cos\theta_2. \tag{2.4}$$

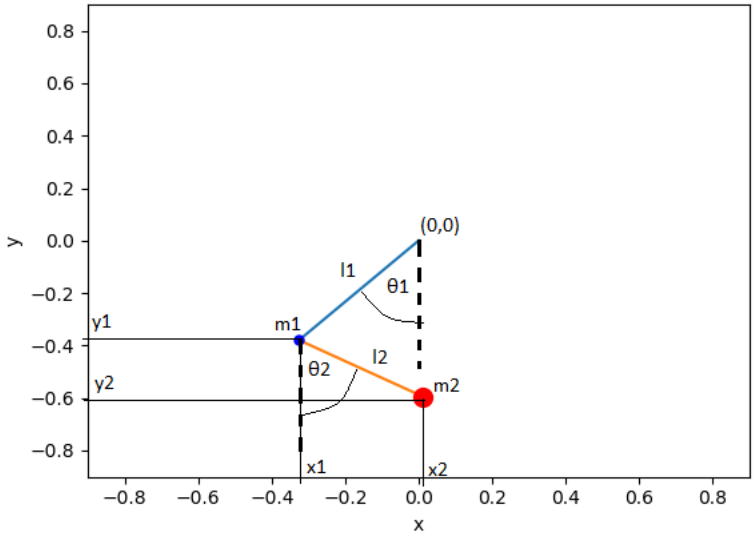

Figure 1: The double pendulum system.

The *Euler-Lagrange equations* determine the evolution of a physical system much like the Newton's laws of motion. The advantage is that they take the same form in any system with generalised coordinates α_i [4]:

$$\frac{d}{dt}\frac{\partial L}{\partial \dot{\alpha}_i} - \frac{\partial L}{\partial \alpha_i} = 0, \tag{2.5}$$

where L denotes the Lagrangian (L = kinetic − potential energy) of the system and $i = 1, 2, ..., n$ for n coordinates. In our case $\alpha_i = \theta_i$ so $n = 2$ with $\dot{\theta}_i$ being the angular velocities.

The Lagrangian of a double pendulum system is [5]:

$$\begin{aligned} L = (m_1 + m_2)\frac{l_1^2\dot{\theta}_1^2}{2} + \frac{m_2}{2}l_2^2\dot{\theta}_2^2 + m_2 l_1 l_2 \dot{\theta}_1\dot{\theta}_2 cos(\theta_1 - \theta_2) \\ +(m_1 + m_2)gl_1 cos\theta_1 + m_2 g l_2 cos\theta_2 \end{aligned} \tag{2.6}$$

Therefore, the nonlinear system of two equations 2.5 governing the motion of our pendulums can be shown to be [5]:

$$\begin{cases} (m_1 + m_2)l_1\ddot{\theta}_1 + m_2 l_2 \ddot{\theta}_2 cos(\theta_1 - \theta_2) + m_2 l_2 \dot{\theta}_2^2 sin(\theta_1 - \theta_2) + (m_1 + m_2)gsin\theta_1 = 0, \\ l_2\ddot{\theta}_2 + l_1\ddot{\theta}_1 cos(\theta_1 - \theta_2) - l_1\dot{\theta}_1^2 sin(\theta_1 - \theta_2) + gsin\theta_2 = 0 \end{cases} \tag{2.7}$$

To create a model of the double pendulum we wish to transform Equations 2.7 into a form which can be easily turned into a numerical integration method. It is required that we deal with first order differential equations. This can be done using the so called *Lagandre transformation* [5]. With it, the Lagrangian (Eq. 2.6) becomes the Hamiltonian: $L(\theta_1, \theta_2, \dot{\theta}_1, \dot{\theta}_2) \longrightarrow H(\theta_1, \theta_2, p_1, p_2)$ where $p_{1,2}$ are called the *generalised momenta* of the two pendulums and [6]:

$$H = \frac{m_2 l_2^2 p_1^2 + (m_1 + m_2) l_1^2 p_2^2 - 2 m_2 l_1 l_2 p_1 p_2 cos(\theta_1 - \theta_2)}{2 m_2 l_1^2 l_2^2 [m_1 + m_2 sin^2(\theta_1 - \theta_2)]} \\ -(m_1 + m_2) g l_1 cos\theta_1 - m_2 g l_2 cos\theta_2. \tag{2.8}$$

Each Lagrange equation of 2.7 becomes a system of two first order differential equations.

The final system of four differential equations of the first order becomes [5]:

$$\begin{cases} f_1 = \dot{\theta}_1 = \frac{p_1 l_2 - p_2 l_1 cos(\theta_1 - \theta_2}{l_1^2 l_2 [m_1 + m_2 sin^2(\theta_1 - \theta_2)]} \\ f_2 = \dot{\theta}_2 = \frac{p_2 (m_1 = m_2) l_1 - p_1 m_2 l_2 cos(\theta_1 - \theta_2)}{m_2 l_1 l_2^2 [m_1 + m_2 sin^2(\theta_1 - \theta_2)]} \\ f_3 = \dot{p}_1 = -(m_1 + m_2) g l_1 sin\theta_1 - A_1 + A_2 \\ f_4 = \dot{p}_2 = -m - 2 g l_2 sin\theta_2 + A_1 - A_2, \end{cases} \tag{2.9}$$

where

$$A_1 = \frac{p_1 p_2 sin(\theta_1 - \theta_2)}{l_1 l_2 [m_1 + m_2 sin^2(\theta_1 - \theta_2]}, \tag{2.10}$$

$$A_2 = \frac{p_1^2 m_2 l_2^2 - 2 p_1 p_2 m_2 l_1 l_2 cos(\theta_1 - \theta_2) + p_2^2 (m_1 + m_2) l_1^2}{2 l_1^2 l_2^2 [m_1 + m_2 sin^2(\theta_1 - \theta_2]^2} sin[2(\theta_1 - \theta_2)]. \tag{2.11}$$

Equations 2.9 are the ones which have been transformed into a numerical integration method (See next Section).

We call $\vec{Z}$ the vector containing the generalised coordinates; $\vec{Z} = (\theta_1, \theta_2, p_1, p_2)$. Then the set of equations in 2.9 can be represented as a function of $\vec{Z}$; $\vec{f}(\vec{Z})$, where $\vec{f} = (f_1, f_2, f_3, f_4)$.

3 Code Description

3.1 4th order Runge-Kutta method of integration

The time evolution of our model has been performed using the 4th order Runge-Kutta method (RK4). At each step n, four vectors are evaluated [5]:

$$\vec{Y_1} = \tau \vec{f}(\vec{Z}_n),$$

$$\vec{Y}_2 = \tau \vec{f}(\vec{Z}_n + \frac{1}{2}\vec{Y}_1),$$
$$\vec{Y}_3 = \tau \vec{f}(\vec{Z}_n + \frac{1}{2}\vec{Y}_2),$$
$$\vec{Y}_4 = \tau \vec{f}(\vec{Z}_n + \vec{Y}_3).$$

Each of these contains information about the slopes of the generalised coordinates at different points between n and $n+1$. τ represents the distance between the two steps. The time evolution is established by setting the value of $\vec{Z}$ at the next step to:

$$\vec{Z}_{n+1} = \vec{Z}_n + \frac{1}{6}(\vec{Y}_1 + 2\vec{Y}_2 + 2\vec{Y}_3 + \vec{Y}_4), \tag{3.1}$$

which uses a weighted average of the slopes found with vectors $\vec{Y}_i$.

3.2 Design

To study double pendulums, two main programs with Python classes have been created.

The *System* class takes two simple pendulum objects defined by their mass and length and uses the Runge-Kutta 4 method to set them in motion. The user needs to define the initial conditions through a 4-element array corresponding to the vector $\vec{Z}$ at time $t = 0$, using a method called set_initial($\vec{Z}_0$). The class also contains a method called motion($\vec{Z}$). It defines all the functions f_1-f_4 from Eq. 2.9 and calculates the vector function $\vec{f}$ using some $\vec{Z}$. This need not be accessed by the user directly. The Runge-Kutta 4 method is implemented by a method called RK(Δt). $\Delta t = \tau$ is the time step which is to be passed in any simulation loop. This method is equivalent to calculating the $\vec{Z}_{n+1}$ in Equation 3.1, where each of the vectors $\vec{Y}_i$ is determined using the motion($\vec{Z}$) method. $\vec{Y}_1$ is calculated with the inital $\vec{Z}_0$ as the argument.

The user can also calculate the hamiltonian of the system (See Eq. 2.8) at any time using the method En_hamiltonian().

Another main piece of code used was a class called *SavePandas* which instantiates a System object (masses and lengths of the pendulums to be passed when initialising) and runs a simulation saving all the relevant information about the system in the meantime. This is done using a method called simulation(steps,timestep,initial conditions) with all the details about the run passed as arguments. Saved are the masses and lengths of the pendulums, the four components of $\vec{Z}$ at each time step and the hamiltonian of the system (See Listing 1). The name of the DataFrame is determined by the user with the save_as(name) method. With the exception of Section 5.4, all of the analysis described in this report is performed using those structures.

A set of plotting functions has been written using an abstract class AbstractDraw to create some of the figures found in this paper. These all use the DataFrames saved

```
import pandas as pd
[...]
[...]
[...]
self.df = pd.DataFrame(self.data,columns=
['TIME','ANGLE_1', 'MOMENTUM_1', 'ANGLE_2',
'MOMENTUM_2', 'HAMILTONIAN','PENDULUM_INFO'])
```

Listing 1: pandas DataFrame saved using a specialised class. Analysis of a double pendulum system can be performed using the contents of such data sets.

with SavePandas, the abstract element being the data plotted. A simple subclass of System containing an analytical solution in the small angle regime called SystemB has been used in Section 5.1. A program which can perform an animation of any saved run has also been written. We do not use it as an analysis tool but links to some animations created can be found in Appendix A.

4 Software tests and limits

4.1 Performance summary

The code has been found to run into problems when the parameters of the pendulums are small. This seems to be due to the functions f_1 and f_2 from the set of equations 2.9 becoming too big. A set of conditions has been implemented to the System class which makes it throw an exception in those cases. This does not solve the problem but provides the user with an idea of what is happening. The exception will be thrown when either of the pendulum's lengths is 10^{-3}m or smaller or if either of the masses reaches 10^{-5}kg or less. This does not rule out all the cases where the program breaks down (For example setting all masses and lengths to 10^{-2}). Fortunately, these cases do not reflect conventional pendulums that we wish to study in this report (Individuals interested in the research of tiny pendulums will not find this software useful).

After recognising these shortcomings, a set of tests has been established using the *pytest* package to ensure the software runs as desired for the analysis. Table 1 summarises them along with their results.

The Hamiltonian of our system describes its total energy and should be a conserved quantity as its form does not explicitly depend on time [4]. Nonetheless, the numerical accuracy of our method is finite and can be influenced by the time step Δt used in a given simulation. The user can ensure a chosen Δt is sufficient for their run by analysing the 'HAMILTONIAN' column in a DataFrame saved with Save_Pandas.

Test	Return
Initialise a System object	Passed
Access the masses and lengths of a System object	Passed
Set initial conditions for a System object	Passed
Access the components of Z_0	Passed
Calculate $\vec{f}$ for a System and compare with predicted values	Passed
Save a simulation using SavePandas	Passed
Access an entry in a saved DataFrame	Passed
Conserve energy	Passed
Reproduce simple harmonic motion (See Section 4.2)	Passed
Reproduce beats (See Section 5.1)	Passed

Table 1: Set of tests for software which models and analyses double pendulum systems.

For example, the simulations in Section 5.4 have been running for up to 1000 seconds. A time step of $\Delta t = 0.002$s has been found to give a $< 1\%$ fractional change in the Hamiltonian for $\vec{Z}_0 = [3, 3, 0, 0]$ and $l_1 = l_2 = 0.1$m over that time. For a similar case with $l_1 = l_2 = 1$m the sufficient Δt was 0.008s to obtain the same result. In both cases, the Hamiltonian was decreasing linearly with time. As all other runs used in this report have been performed on much shorter time scales with similar pendulums, we conclude that the software conserves energy well for most purposes.

An important takeout is that the scale of the pendulums used and the time of the simulations can be some of the factors which determine the accuracy of a run.

4.2 Simple Harmonic Motion

By setting $m1$ to a tiny number ($m_1 = 10^{-4}$) and displacing both pendulums initially by the same small angle $\theta_1 = \theta_2 = 0.1$ rad, the simple harmonic motion of a single pendulum has been reproduced. This is a periodic motion with period:

$$T = 2\pi\sqrt{\frac{l}{g}} \tag{4.1}$$

where l in our case is $l_1 + l_2$. The angle of such pendulum will change with time as $\theta = cos(\frac{2\pi}{T}t)$. The lengths have been set to $l1 = l2 = 0.5$ m, resulting in $T = 1.987$ s. The simulation data agrees with the prediction as seen in Figure 2. This result is evidence of proper implementation of the numerical method.

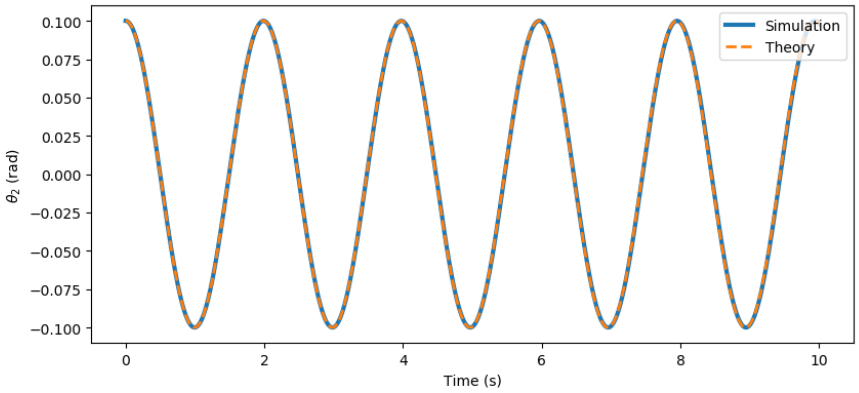

Figure 2: Simple harmonic motion reproduced in a double pendulum system by making the mass of the first pendulum negligible and displacing both parts by the same amount. This mimics a single pendulum of length $l = l_1 + l_2$.

5 Double pendulum

5.1 Beats

In the small angle regime ($\theta_1 \wedge \theta 2 << 1$), an analytical solution for the double pendulum can be found (without imitating a single pendulum). This can be thought of as another test for the code, but it is also a phenomenon worth mentioning.

If the lengths of the two pendulums are equal and $Z_0 = [0, \theta_{2,0}, 0, 0]$ then the angles of the system follow the equations [5]:

$$\theta_1(t) = \frac{\theta_{2,0}}{2}\sqrt{\frac{\mu}{1+\mu}}(-cos(\omega_1 t) + cos(\omega_2 t)), \tag{5.1}$$

$$\theta_2(t) = \frac{\theta_{2,0}}{2}(cos(\omega_1 t) + cos(\omega_2 t)), \tag{5.2}$$

where $\mu = \frac{m_2}{m_1}$ and

$$\omega_{1/2}^2 = \frac{g}{l}[1 + \mu \pm \sqrt{(1+\mu)\mu}]. \tag{5.3}$$

A simple subclass of System called SystemB has been created to include Equations 5.1 and 5.2. Figure 3 shows the predicted and simulated angle of the first pendulum as a function of time, providing another proof of the code's functionality.

If we define $\bar{\omega} = \frac{\omega_2+\omega_1}{2}$ and $\Delta\omega = \frac{\omega_1-\omega_2}{2}$ then $\omega_\pm = \bar{\omega} \pm \Delta\omega$. Then using appropriate trigonometric identities it can be shown that:

$$\theta_1(t) = -\theta_{2,0}\sqrt{\frac{\mu}{1+\mu}}sin(\bar{\omega}t)sin(\Delta\omega t), \tag{5.4}$$

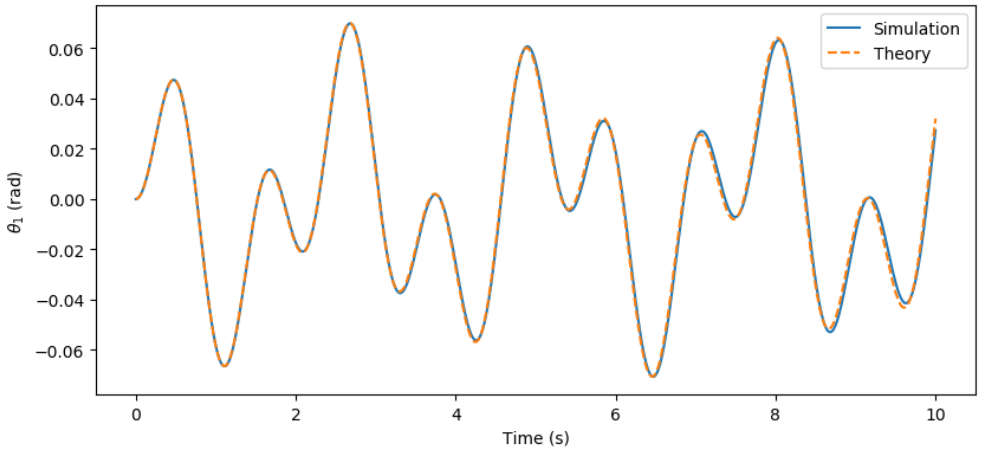

Figure 3: A double pendulum model produces the phenomenon of beats in the small angle regime using numerical integration.

$$\theta_2(t) = \theta_{2,0} cos(\bar{\omega}t) cos(\Delta\omega t). \tag{5.5}$$

This can be considered as oscillations at the higher frequency $\bar{\omega}$ with a periodic amplitude modulation $\Delta\omega$. The amplitude modulation is $\frac{\pi}{2}$ radians out of phase for the two bobs. This means that when one of them experiences maximum suppression, the other is minimally suppressed. Energy is transferred from one pendulum to the other in the form of beats. Figure 4 shows this behaviour for different values of μ.

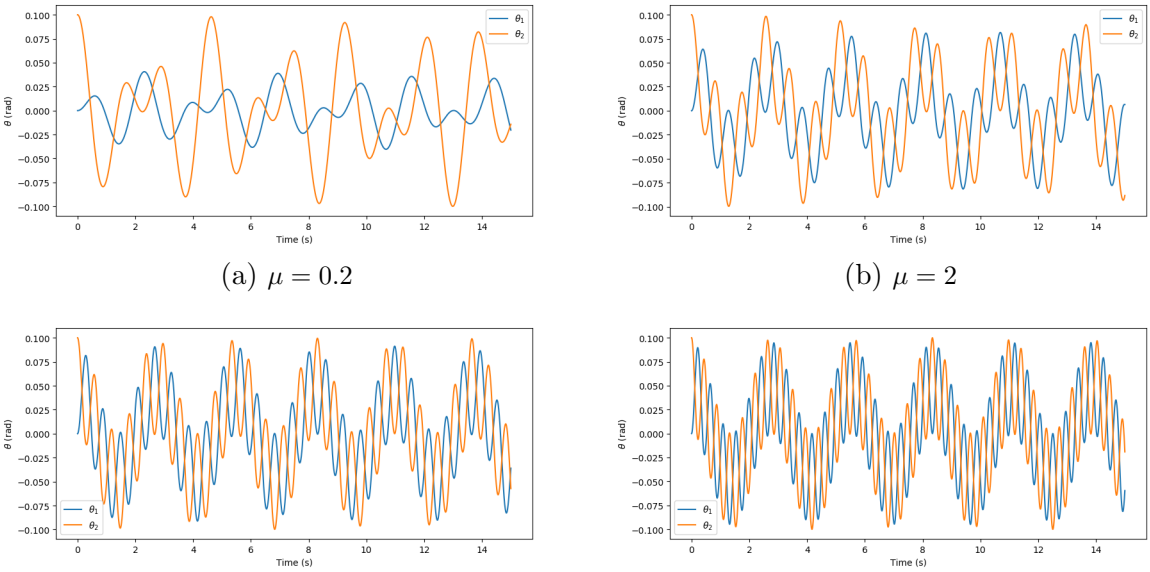

(a) $\mu = 0.2$ (b) $\mu = 2$

(c) $\mu = 5$ (d) $\mu = 10$

Figure 4: The phenomenon of beats for different mass ratios (μ) of the two pendulums. The higher the ratio the more prominent the periodic energy transfer becomes.

5.2 Initial Conditions Sensitivity

The main aspect of chaos is the lack of predictability of the system's time evolution under small initial condition changes. We showcase that for the double pendulum by comparing the paths taken by two bobs with a slight difference in their initial displacement.

Consider the trajectories of the second bob for the two cases: $Z_{0,1} = [\frac{\pi}{2}, 1.9, 0, 0]$, $Z_{0,2} = [\frac{\pi}{2}, 1.905, 0, 0]$ shown in Figure 5. The simulation was run for 10 seconds and as seen in 5b the paths are identical for about 6 seconds but diverge significantly afterwards. After 10 seconds the paths appear completely unrelated and one would not expect them to have started from a nearly identical setup. This feature makes it impossible for chaotic systems to be "traced back in time", even though the equations governing them are well known. This is the idea of *deterministic chaos* [1]. Even though the exact evolution of a system is uniquely dependent on the initial conditions and could theoretically be tracked, measurement or roundoff errors will always occur and they can easily lead to a complete unpredictability of the measured system [7].

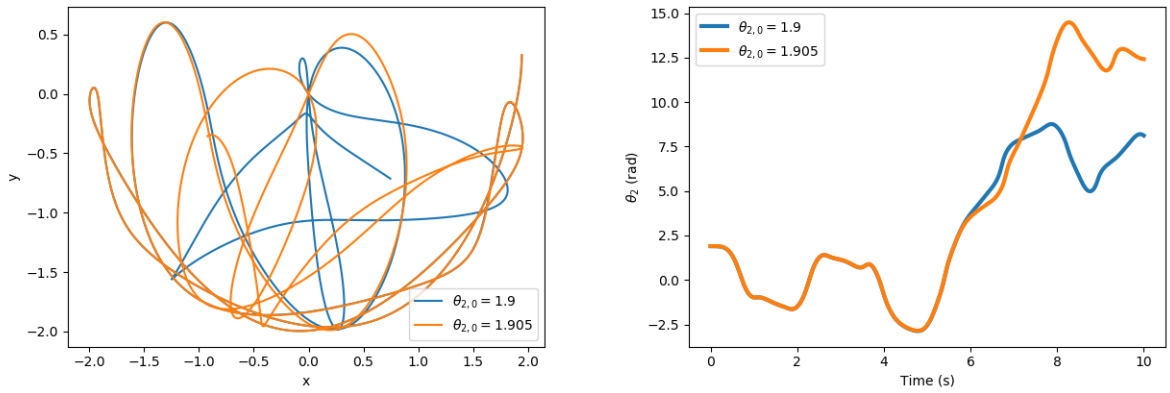

(a) The paths taken by the bobs.

(b) The angle evolution with time.

Figure 5: Small difference in the initial displacement of one of the bobs of a double pendulum leads to a significant divergence of paths after just 10s.

5.3 Energy-dependent chaos

As shown before, the double pendulum system exhibits predictable, analytical behaviour in the small angle regime. We know that it can also produce chaotic motion for other initial conditions. We further investigate the system by looking at its evolution at different energies. For this part we work with unit masses and lengths; $m_1 = m_2 = l_1 = l_2 = 1$ (kilograms and meters respectively). To do so, a program which "scans" through some part of the available phase space has been written. Angles have been varied from 0.1 to π radians and the momenta from 0 to 10 $\frac{\text{kg m}^2}{\text{s rad}}$ (Notice the unusual units for the generalised momentum), giving a total of 2442 unique simulations run for 30 seconds each. To investigate the behaviour, each simulation has been plotted in the phase space for the first pendulum (p_1 versus θ_1 graphs). I propose five distinct categories of the evolution based on the shape of the phase space path and investigate the energy distribution of each category.

5.3.1 A - Quasiperiodic

These graphs show a significant level of stability. The notion of *quasiperiodic* motion is adapted [8], roughly meaning the paths taken over some period are close to one another, but not identical. Figure 6 shows some examples of such cases. Runs like the one in Fig. 6d appear very close to being completely periodic. On the other hand, some, like the one in Fig. 6h could be argued to be chaotic and belong to the next category. Borderline cases like this arise from the very empirical and purely visual nature of my analysis. Overall though, the number of such examples is not a significant percent of the total in each category and therefore does not spoil the overall conclusions.

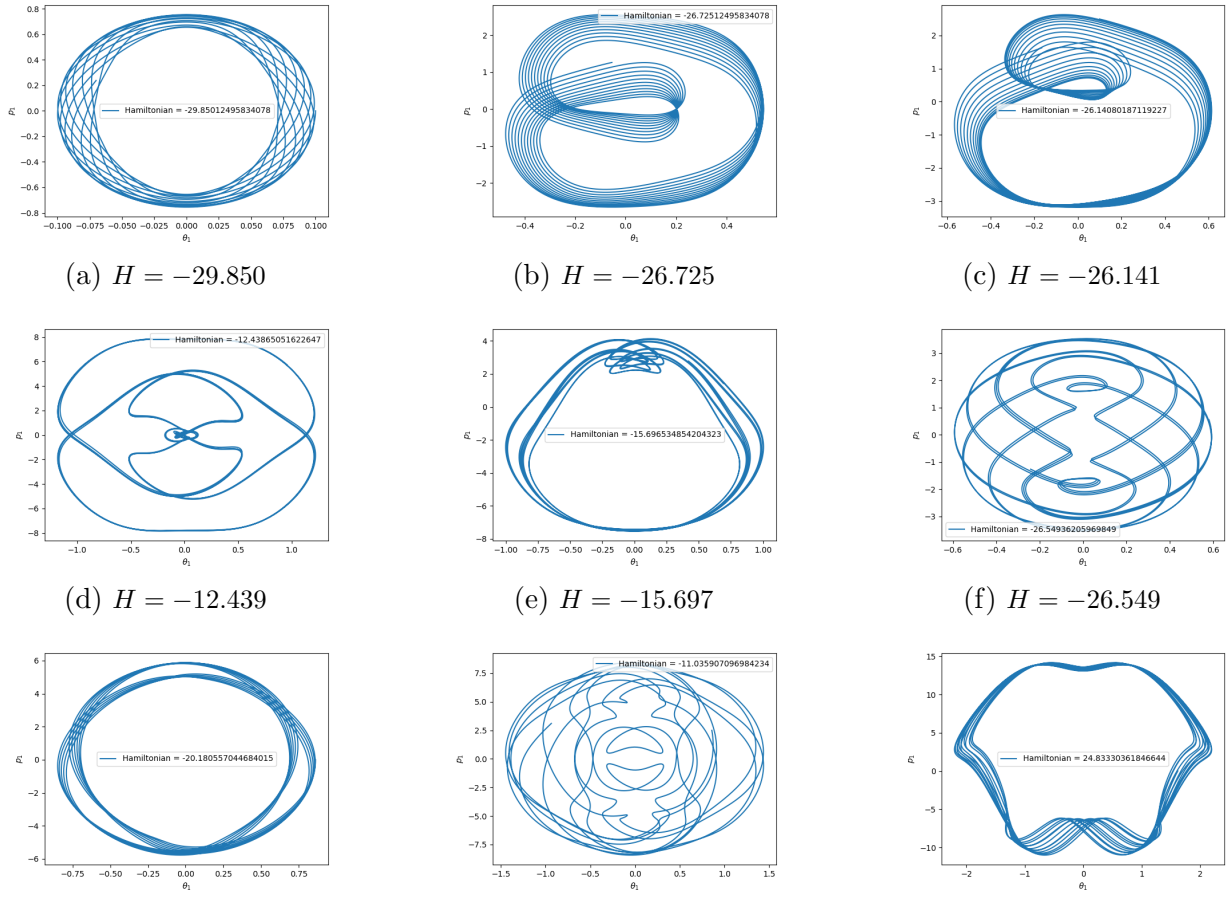

(a) $H = -29.850$ (b) $H = -26.725$ (c) $H = -26.141$

(d) $H = -12.439$ (e) $H = -15.697$ (f) $H = -26.549$

(g) $H = -20.181$ (h) $H = -11.036$ (i) $H = 24.833$

Figure 6: Examples of quasiperiodic phase space paths of one of the bobs of a double pendulum.

5.3.2 B - Chaotic with no flip

These runs do not show any significant periodicity - the paths appear random and chaotic. The pendulum does not perform a flip during the run, meaning that the path does not extend beyond π radians on the horizontal axis. Notice how 7c shows resemblance to 6d. They both appear at similar energies (-11.433 and -12.439 Joules respectively), indicating that there exist certain initial conditions which result in a more stable path from which similar but increasingly chaotic paths diverge.

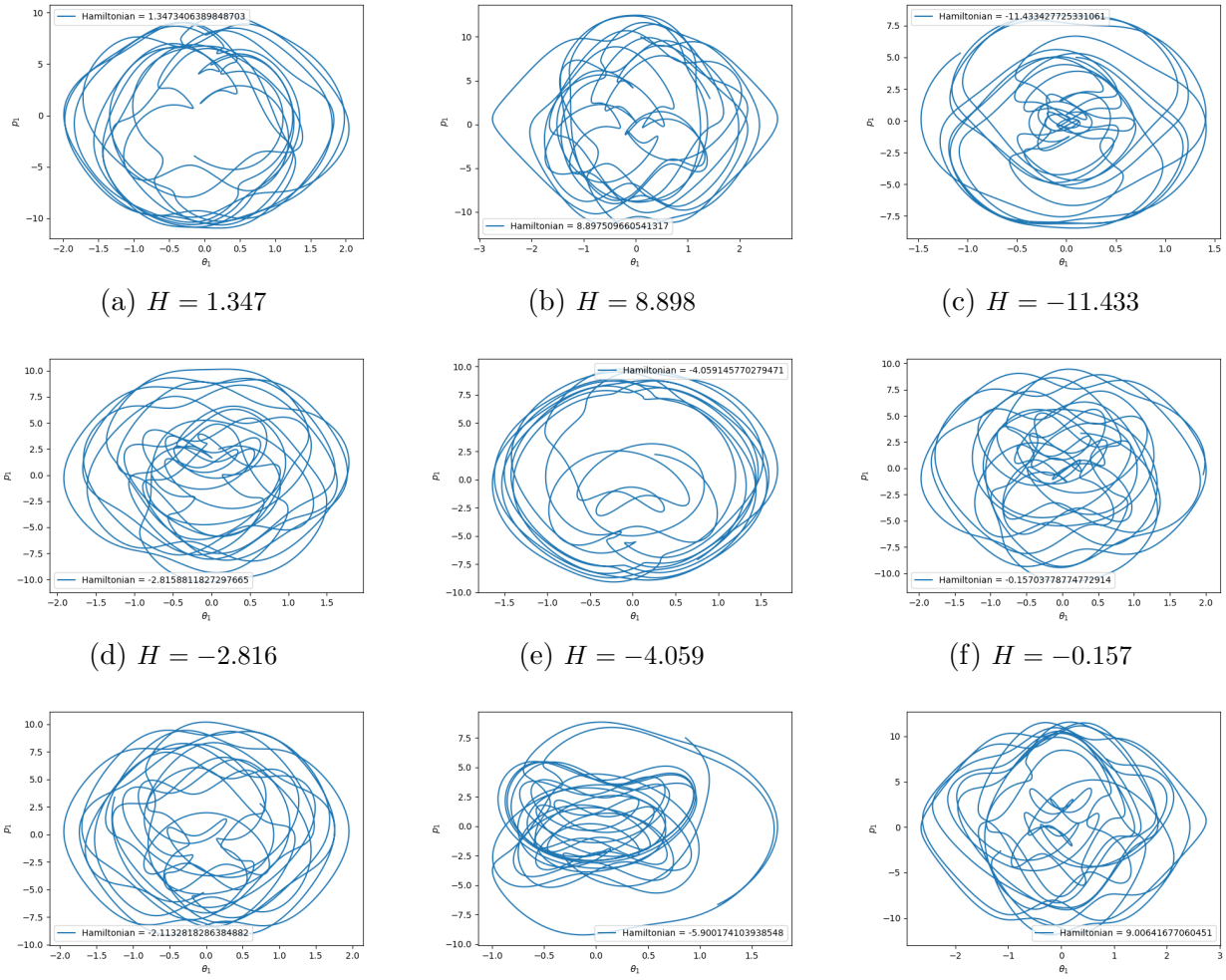

(a) $H = 1.347$ (b) $H = 8.898$ (c) $H = -11.433$

(d) $H = -2.816$ (e) $H = -4.059$ (f) $H = -0.157$

(g) $H = -2.113$ (h) $H = -5.900$ (i) $H = 9.006$

Figure 7: Phase space paths exhibiting chaotic behaviour without performing a flip.

5.3.3 C - Chaotic with flips

These paths are also defined by irregular, chaotic motion, but the pendulum performs at least one flip, meaning the graphs extend beyond π radians. Several flips may occur (path reaching over multiples of π on the angle axis) but overall the motion is dominated by the chaotic behaviour and does not tend to continuously diverge from the origin. This means that the average angular velocity is roughly 0. A good example of that is 8f, where the pendulum started to spin in the negative angle direction but reached some maximum angle and began to "unwind" in the opposite direction.

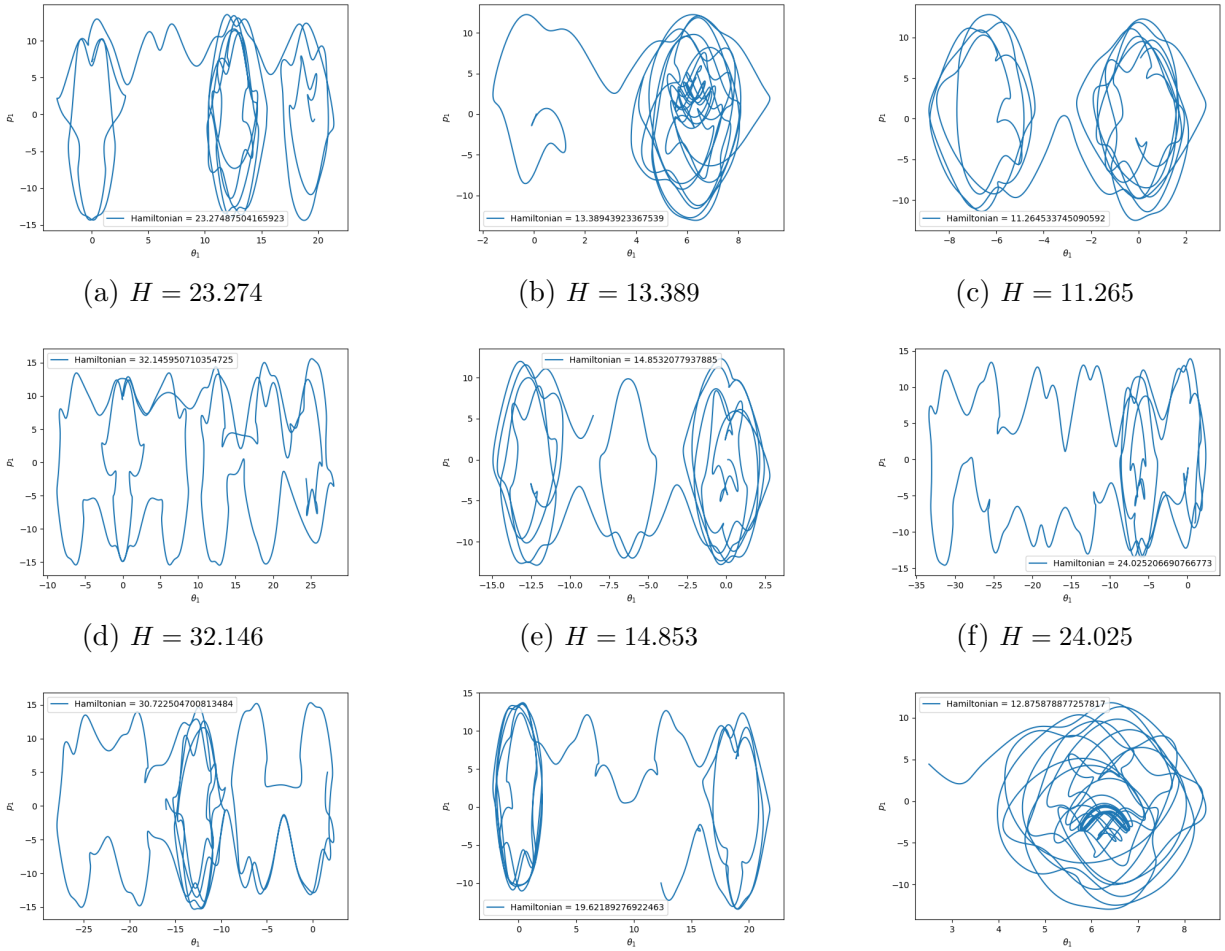

(a) $H = 23.274$ (b) $H = 13.389$ (c) $H = 11.265$

(d) $H = 32.146$ (e) $H = 14.853$ (f) $H = 24.025$

(g) $H = 30.723$ (h) $H = 19.622$ (i) $H = 12.876$

Figure 8: Chaotic behaviour with at least one pendulum flip.

5.3.4 D - Chaotic with spinning

This category consists of cases where the spinning motion takes over the chaotic behaviour. The unpredictable paths can still be found but overall the tendency for the pendulum is to continue rotating in one direction. There are cases like 9c, 9g and 9i where the paths almost become periodic. These are some of the most energetic cases. There, the kinetic energy of the angular motion becomes much more significant than the gravitational potential energy of the system, and the angular momentum can be considered to be conserved as the torque from gravity vanishes [9].

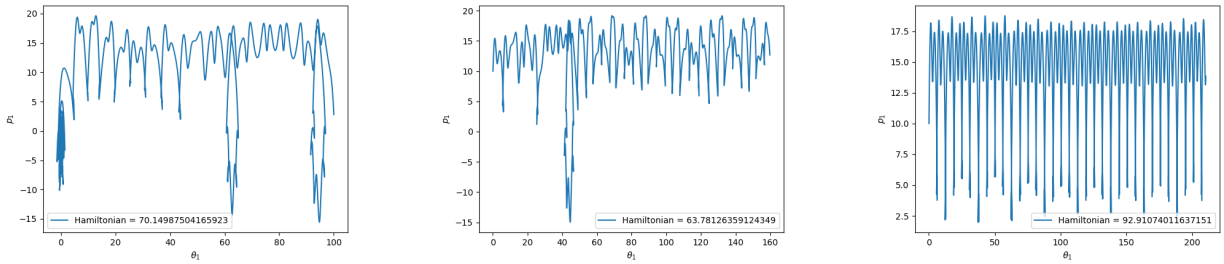

(a) $H = 70.150$ (b) $H = 63.781$ (c) $H = 92.911$

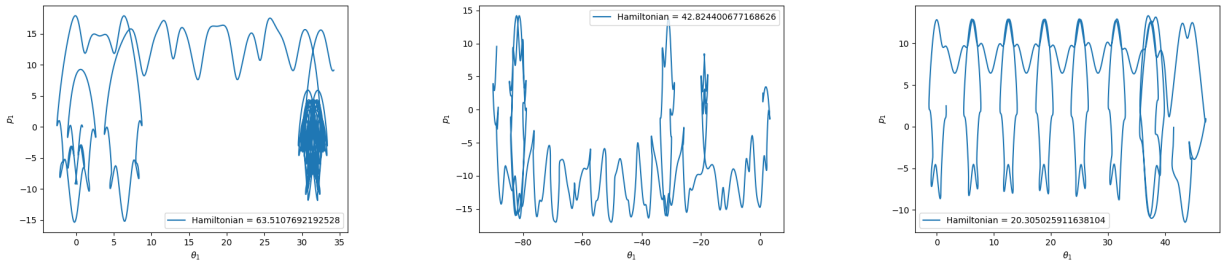

(d) $H = 63.511$ (e) $H = 42.824$ (f) $H = 20.305$

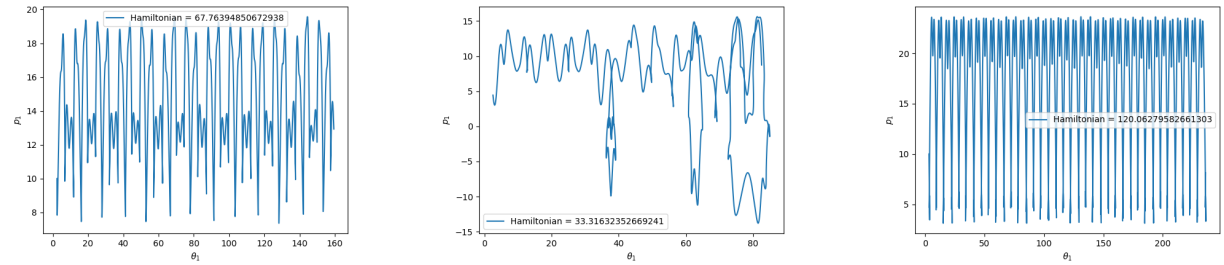

(g) $H = 67.764$ (h) $H = 33.316$ (i) $H = 120.062$

Figure 9: Highly energetic double pendulums. The pendulum starts spinning in one direction.

5.3.5 E - High energy quasiperiodic

The last category is an interesting one. We again see quasiperiodic motion, but it occurs at higher energies and the patterns are vastly different to the ones in category A. These cases are extremely rare (only 12 instances found) and seem to usually occur when initially, the first pendulum is not displaced significantly ($\theta_1 = 0.1$ rad) and the second pendulum is displaced maximally ($\theta_2 = \pi$). Exceptions like 10a ($\theta_1 = \theta_2 = 0$) occur nonetheless.

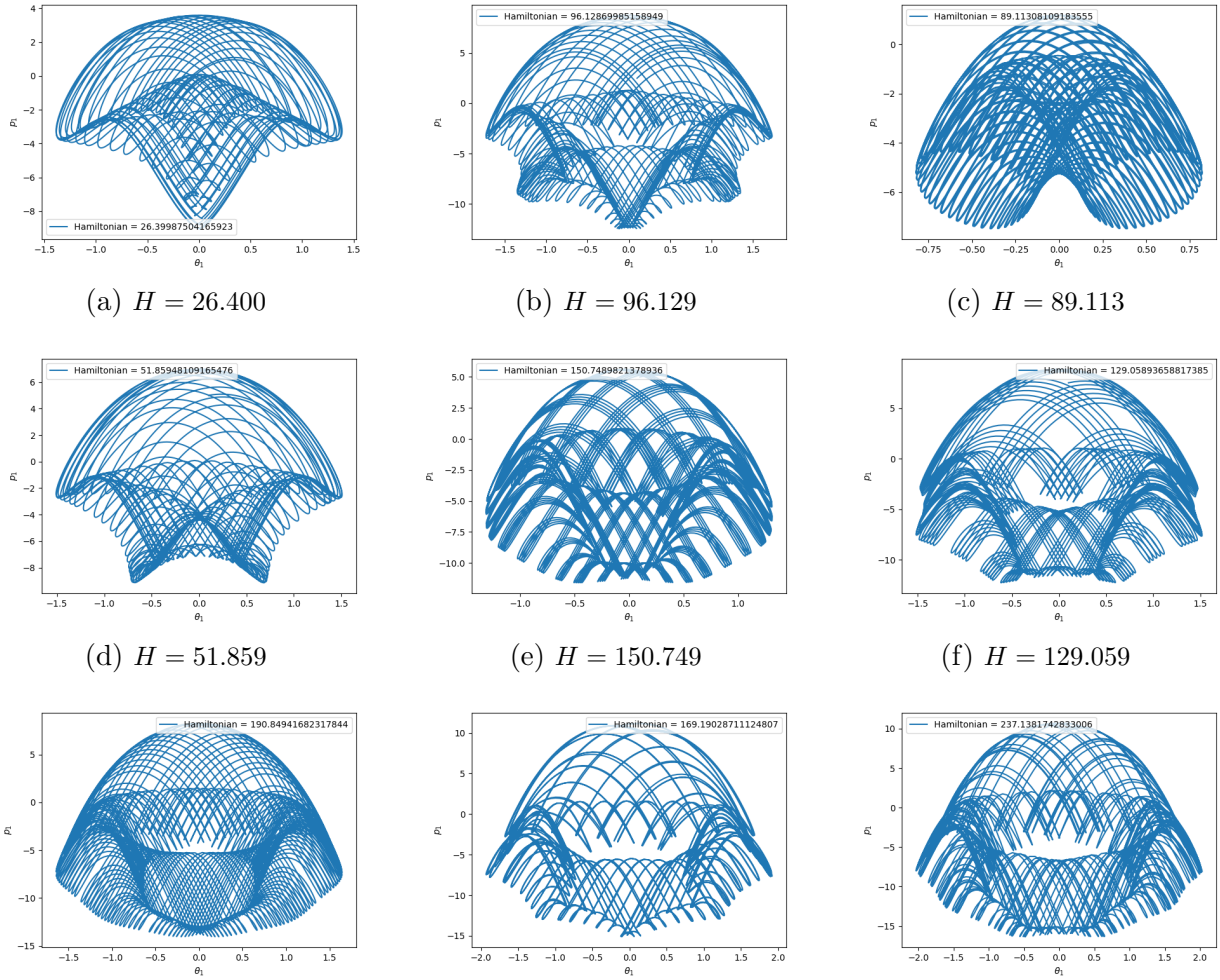

(a) $H = 26.400$ (b) $H = 96.129$ (c) $H = 89.113$

(d) $H = 51.859$ (e) $H = 150.749$ (f) $H = 129.059$

(g) $H = 190.850$ (h) $H = 169.190$ (i) $H = 237.138$

Figure 10: Rare quasiperiodic patterns for highly energetic double pendulums.

5.3.6 Energy spectrum

A histogram of energies has been found for each of the categories, therefore creating an energy spectrum of the pendulum behaviour (See Figure 11). Category A dominates over the range $-30 \leq H \leq -10$J. Next, over $-10 \leq H \leq 10$ J, most runs belong to category B. $10 \leq H \leq 25$ J is mostly populated by category C. Above 25 joules most initial conditions end up drawing D paths. The rare E cases show up throughout most of the high energy range ($\approx$ 20-250 J). The main takeout from this experiment is that even though the individual paths can differ significantly, there are certain common features that we can expect at different energy ranges. Nonetheless, it is important to remember that there is a significant level overlap between the categories and stable configurations can be found "next to" chaotic ones.

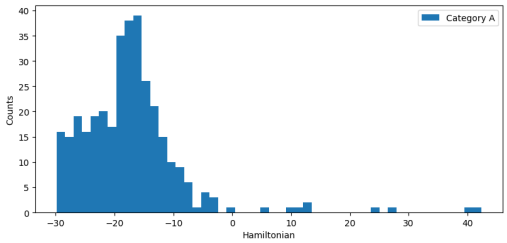

(a) Category A

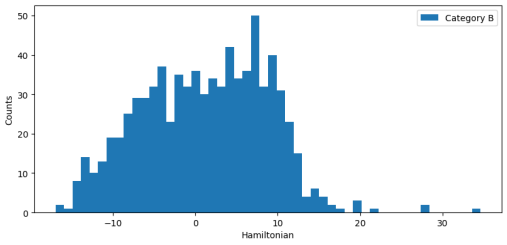

(b) Category B

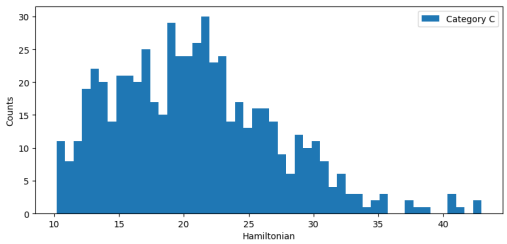

(c) Category C

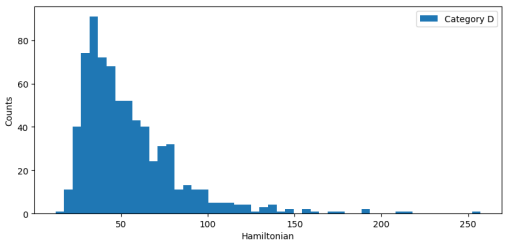

(d) Category D

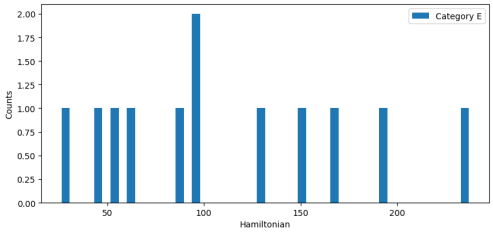

(e) Category E

Figure 11: Energy histograms for five categories of motion of the double pendulum system.

5.4 Flipping time

The final piece of our analysis has to do with the time it takes for the system to flip as a function of the initial conditions. That is, how long it takes for either θ_1 or θ_2 to reach a value greater than π.

There is no analytical solution for when a bob performs a flip, apart from when the system does not have enough energy - then it never happens. Let us consider what are the constraints on the initial conditions for that case. The potential energy U in the Hamiltonian (Eq. 2.8), when the masses are the same ($m_1 = m_2 = M$) and so are the lengths ($l_1 = l_2 = L$) is:

$$U = -MgL2cos(\theta_1 + \theta_2). \tag{5.6}$$

For this part of the report, only the initial angles have been varied, keeping the momenta equal to 0 such that, at the beginning, all of the system's energy is potential. Minimal initial energy must be greater than either of the following total energies associated with one of the bobs flipping: when $\theta_1 = 0$ and $\theta_2 = \pi$ or $\theta_1 = \pi$ and $\theta_2 = 0$. Pendulums have 0 momentum in both cases for the minimal condition. Turns out that the energy associated with the former is smaller and we use that as our energy constraint, obtaining:

$$2cos(\theta_1) + cos(\theta_2) = 1. \tag{5.7}$$

We call the space inside this curve the *forbidden region*. Points outside have enough energy to flip. I represent the data as a colour map in Figure 12. Each of the 40000 points represents different starting conditions in the range $-\pi < \theta_{1,2} < \pi$. The white area corresponds to the forbidden region and intricate patterns can be seen outside of it, showcasing the complexity of the double pendulum motion. The mapping is done with a logarithmic scale, meaning that flips can occur at times of several different orders of magnitude. The natural timescale for a pendulum is $T_0 = \sqrt{\frac{l}{g}}$ (Scale associated with the period of its simple harmonic motion). We have used pendulums of lengths 0.1cm which results in $T_0 = 0.1$. Several regions of similar behaviour are revealed, especially towards the edges of the figure, represented by shapes of like shade with "fuzzy", unpredictable regions in between.

A symmetry with respect to the origin is expected, meaning that for a point P on the map: $P(\theta_1, \theta_2) = P(-\theta_1, -\theta_2)$ in theory. A numerical precision estimate can be performed by subtracting the values on opposite points of the origin. Each simulation was run with a $\Delta t = 0.002$s time step and lasted up to 1000s. Any discrepancy detected was recorded as a relative error $\Delta t_f(P, -P)$:

$$\Delta t_f(P, -P) = \left| \frac{t_f(P) - t_f(-P)}{t_f(P)} \right| \times 100\%. \tag{5.8}$$

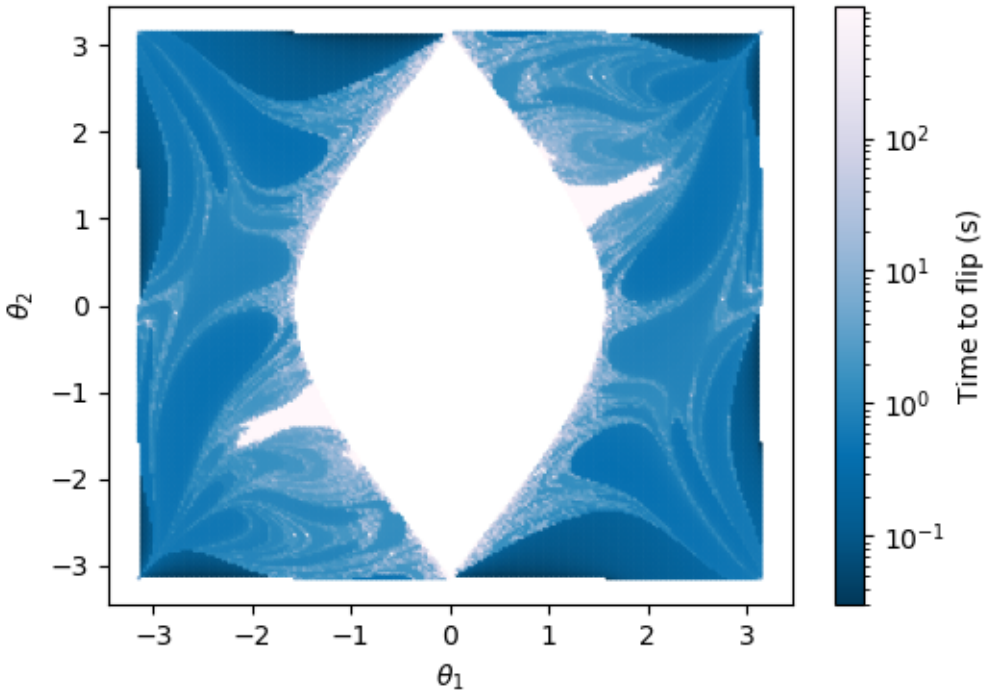

Figure 12: Double pendulum flipping time. The colour map has a logarithmic scaling with the natural timescale for the pendulum $T_0 = 10^{-1}$s. The white area in the middle of the figure represents the forbidden region.

The results can be seen in Figure 13. Most pairs of points gave the same results, but a region just outside the forbidden zone has produced 390 (or 195 pairs of) points with discrepancies up to about 10%. The nearest neighbourhood of the forbidden zone is where a lot of "fuzziness" is present (big sensitivity to initial conditions). It is also where the average time to flip appears the longest. Longer simulations have more time to accumulate any numerical precision error. Overall, only less than 1% of the points on the map produced noticeable errors. These points occur on the most chaotic and long-running parts of the graph. I therefore conclude that the data used in Fig. 12 provides a good representation of the double pendulum flip time up to a precision of 0.002s (the time step of the simulation).

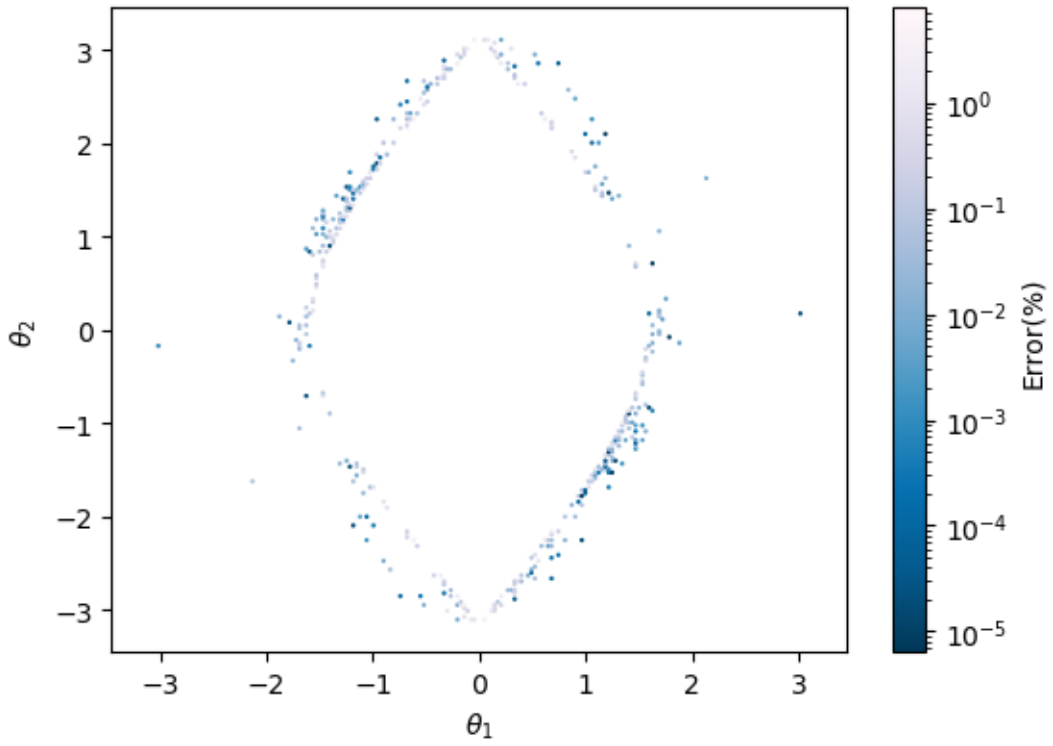

Figure 13: Relative error on the data points based on the symmetry postulate. The discrepancies appear mainly on the edge of the forbidden zone where the time to flip was the largest and where large initial condition sensitivity occurs.

6 Conclusions

A set of Python programs which allow the user to create simulations of the double pendulum system have been written. The 4th order Runge-Kutta method of numerical integration has been implemented in order to perform the time evolution of the system and pandas' DataFrames have been used to store simulation data. The code has passed several simple tests and has shown to reproduce analytically-solvable cases as expected. The total energy decreases linearly with time in a given simulation yet for most runs the accumulative loss is negligible and the energy can be considered to be conserved. It is important that the user picks an appropriate time step for the integration depending on the scale of the pendulums.

The phenomenon of beats has been investigated in the small angle regime and has been shown to be the most prominent at the largest value of the bob mass ratio: $\mu = 10$. The divergence of two bob paths with initial conditions $\theta_{2,0} = 1.900$ and $\theta_{2,0} = 1.905$ was described. The two trajectories remained nearly identical for about 6 seconds but were completely unrelated after just 10s, owing to the chaotic nature of double pendulums. Five general categories of motion have been proposed by the author as an attempt to get a more statistical, systematic view of the double pendulum behaviour. An energy range relating to each category has been found, albeit with a significant level of overlap.

Finally, a colour map has been created, visualising the time it takes for either of the bobs to perform a flip ($\theta > \pi$). Rich, intricate patterns were observed with several regions of common behaviour and more chaotic, fuzzy spaces in-between. The numerical precision of the program has also been tested using a theoretical postulate about symmetry of the data. It has been found to be over 0.002s for about 99% of the points with only the longest (100-1000s) and most sensitive runs producing ambiguous results with differences in flip time up to about 10%.

I believe that the code can be used as a great analysis tool for the motion of double pendulums as well as an introductory study of chaos. Further investigations could improve on the generality of the system in question by accounting for driving or damping in the equations of motion.

References

[1] Williams G P, National Academy of Sciences, *Chaos Theory Tamed*. Washington: National Academies Press; 1997. Chapters 1-2.

[2] Mihailovic D, Mimic G, Arsenic I. Climate Predictions: The Chaos and Complexity in Climate Models. Advances in Meteorology. 2014;2014:1-14.

[3] Skiadas C H, Dimotikalis I, *Chaotic systems theory and applications*. World Scientific; 2010.

[4] Liberzon D, Calculus of variations and optimal control theory: a concise introduction. Princeton University Press; 2012. Chapter 2 Calculus of variations.

[5] Svirin, A. *Double Pendulum*. Available from: https://www.math24.net/double-pendulum/. Lagrange Equations. [Accessed 17/04/2020]

[6] Assencio D. *The double pendulum: Hamiltonian formulation* Available from: https://diego.assencio.com/?index=e5ac36fcb129ce95a61f8e8ce0572dbf. [Accessed 17/04/2020]

[7] Williams G P, National Academy of Sciences, *Chaos Theory Tamed*. Washington: National Academies Press; 1997. Chapter 14 Sensitive dependence on initial conditions.

[8] Magnitskii N A, Sidorov S V, *New methods for chaotic dynamics*. World Scientific; 2006.

[9] Biglari H, Jami A. The Double Pendulum Numerical Analysis With Lagrangian and the Hamiltonian Equation of Motion. 2016

A Links to animations

Example 1 - beats: https://www.youtube.com/watch?v=S_j3Bas3UHQ Example 2: https://www.youtube.com/watch?v=V9fsyYCnx-4 Example 3 - This is a high energy quasiperiodic case (Category E): https://www.youtube.com/watch?v=1dyCrg9nBYY